Lasers in Surgery and Medicine 26:130–144 (2000)

Evaluation of Cooling Methods for Laser Dermatology

H.H. Zenzie, MS,[1]* G.B. Altshuler, PhD,[1] M.Z. Smirnov, PhD,[2] and R.R. Anderson, MD[3]

[1]Palomar Medical Products, Inc., Burlington, Massachusetts 01803
[2]Institute of Fine Mechanics and Optics Laser Center, St. Petersburg 197101, Russia
[3]Massachusetts General Hospital, Wellman Laboratories of Photomedicine, Boston, Massachusetts 02114

Background and Objective: **Skin cooling is used to protect the epidermis in a variety of laser dermatology procedures, including leg vein treatment, hair removal, and port wine stain removal. Spray and contact cooling are the two most popular methods, but similarities and differences of these techniques are not well understood.**
Study Design/Materials and Methods: **A theoretical model of skin cooling is presented for two different regimens: "soft" cooling in which freezing of the skin is not permitted and "hard" cooling in which the skin can be frozen to a given depth. Spray and contact cooling were also compared experimentally using an in vitro model.**
Results: **For a fixed skin surface temperature, spray and contact cooling theoretically produce the same cooling profile in the skin. Anatomic depth of cooling depends on the time for which either the spray or contact is applied. In vitro experiments caused temperature at the simulated basal layer to be between –5 and +5°C for both spray (tetrafluoroethane, boiling point –26°C) and contact (–27°C sapphire plate) cooling. The theoretical precooling analysis shows hard mode to be faster and more selective than soft mode; however, cooling time for hard mode must be carefully controlled to prevent irreversible epidermal damage caused by freezing.**
Conclusions: **Both spray and contact cooling provide efficient skin cooling. The choice of cooling method depends on other factors such as the target depth, cost, safety, and ergonomic factors. Lasers Surg. Med. 26:130–144, 2000** **© 2000 Wiley-Liss, Inc.**

Key words: contact cooling; cryogen spray cooling

INTRODUCTION

Skin cooling is a process we experience everyday; air or water touching the body is typically cooler than core temperature. As a result, the skin surface temperature is typically less than internal body temperature (36.6°C) and ranges from 27–32°C. Brief contact with very cold air or water does not cause skin injury. It is possible for live tissue to survive a certain amount of freezing and thawing [1]. In tissue, electrolytes and solutes reduce the freezing temperature. Freezing can start at tissue temperatures between 0 and –15°C. Theoretically, tissue is solid state when its temperature has passed below the lowest eutectic point of its electrolytes [2].

Contact skin cooling by using ice or chilled gels has been used for anesthesia in dermatologic surgery for many years. Spray coolants are used both for anesthesia and cryosurgery [3]. A third method of skin cooling uses chilled water or gas flow across the skin surface. With the recent introduction of high-energy visible and near-infrared lasers that heat targets well beneath the skin surface, skin cooling has become an area of active clinical and research interest. Light absorption by melanin causes epidermal damage, which limits the maximum fluence that can be used in these procedures. Cooling partially pro-

*Correspondence to: H.H. Zenzie, MS, Palomar Medical Products, Inc., 82 Cambridge Street, Burlington, MA 01803.

Accepted 19 October 1999

tects the epidermis, which permits higher fluences to be delivered to the skin. At present, skin cooling is used for procedures such as photoepilation [4], treatment of port wine stains [5,6], and nonablative skin resurfacing [7]. The principal benefit of these methods for photodermatologic procedures is the spatial selectivity of the cooling. Ideally, the epidermal temperature should be significantly but harmlessly decreased by the cooling procedure, while the target (e.g., blood vessel, stem cells, or matrix cells of the hair follicle, etc.) temperature should remain unchanged or change insignificantly. If the latter condition is not met, the laser fluence must be increased to compensate for the lower target temperature. Thus, the cooling process should ideally be nonstationary (dynamic) in character. References 8–12 provide background material on spray and contact cooling, respectively.

In a recently published paper by Anvari et al., these two methods were compared theoretically and experimentally [13]. However, the comparison was deficient in three respects. First, the theoretical analysis used a Robin boundary condition that assumed a time-independent heat transfer coefficient and a time/coordinate-independent cooling agent (CA) temperature. This boundary condition is appropriate for dynamic cooling. In this case, the heat transfer coefficient must be time dependent, not independent as in previous studies [8,9,10,13]. Additional detail concerning the boundary conditions and heat transfer coefficient are given in Appendix A. Second, the experimental study measured skin surface temperature dynamics through the use of infrared radiometry. This indirect method is very sensitive to compounds (e.g., ice, water, spray liquid, etc.) present on the skin surface in the range of wavelengths used. In addition, Reference 13 compares skin-surface temperatures produced by spray and contact cooling, but clinically the most important site to determine skin temperature is the basal cell layer of epidermis. The basal layer contains a high melanin concentration and is, therefore, the most susceptible site for laser injury of epidermis. Third, Anvari et al. compared contact and spray cooling at very different temperatures: the sapphire contact cooler was maintained at 6–12°C while the liquid spray was tetrafluoroethane (TFE), which boils at −26°C at 1 atm. The study's conclusion that spray cooling was far more effective than contact cooling is not valid when the initial sapphire temperature is properly chosen.

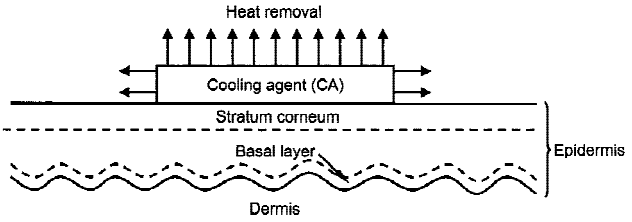

Fig. 1. Skin cooling schematic.

In this study, we compare the two cooling techniques by using more appropriate theoretical and experimental methods. Several regimens of epidermal protection are also described: precooling, parallel cooling, and optical damping. For the case of skin precooling, spray and contact cooling are compared theoretically under ideal conditions. A theoretical model of parallel cooling and the conditions required to derive benefit from this cooling method is also presented. In the experimental section, direct temperature measurements are made at the depth of dermal/epidermal junction in an in vitro model, for both contact and spray cooling.

MECHANISMS OF SKIN COOLING

All methods of skin cooling remove heat from the skin to a contact CA such as gas, liquid, or a low-temperature solid (Fig. 1). The CA may move along the surface of the skin, as in the case of a flowing gas or liquid, or a moving solid. In this case, heat removal from the skin is aided by mass transfer of the heated CA. Hereafter, we consider the CA to be stable during the cooling cycle, which is true in the case of heat removal by conductive cooling. For spray cooling, the CA is a liquid whose temperature is lower than surface skin temperature. Heat is removed from the skin into the CA by conduction, but heat is removed from the liquid CA by evaporation. Thus, spray is simply a different type of contact cooling in which rapid evaporation cools the CA. For spray, the contact layer evolves in time as the liquid boils and evaporates. For solid contact cooling, there may be either active or passive heat removal from the CA. The active CA is typically a solid with high thermal capacity and thermal conductivity, cooled by flowing liquid, gas, spray, or thermoelectric elements. In this way, the average CA temperature is constant. In the passive case, there is no active heat removal from the CA, which results in an average temperature rise after contact with skin. As an example, cold gel is a

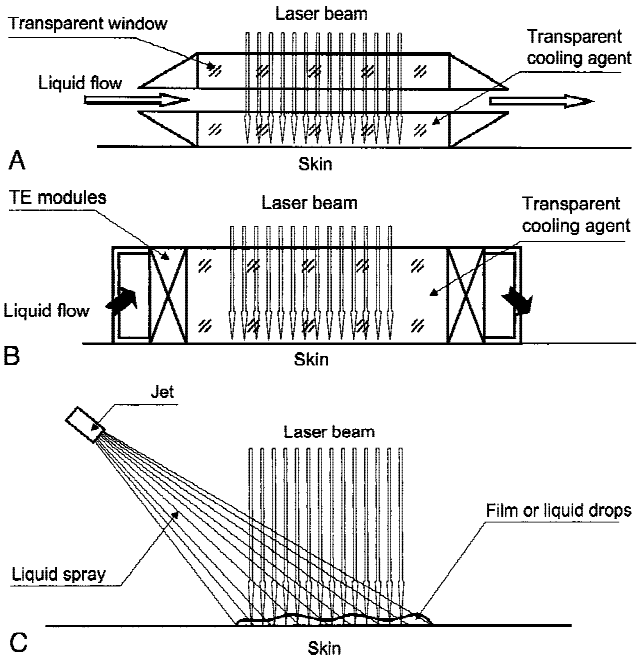

Fig. 2. **A,B:** Two implementations of contact plate cooling with active heat removal. **C:** Typical implementation of spray cooling.

passive cooler. Hereafter, we consider only active contact and spray cooling.

Figure 2 shows typical skin coolers used in laser dermatology. Laser light must pass through the CA during treatment. Among solids, sapphire is nearly ideal for contact cooling. Sapphire is transparent in the 0.2–5 μm wavelength range, has a high optical damage threshold, and is close to metal with respect to its thermal conductivity. Hereafter, we consider a contact cooler based on this "optical metal." The principal difference between the contact coolers shown in Figure 2A and B is the method used to remove heat from the sapphire. The cooler shown in Figure 2A is designed with liquid flow across the light beam. In this case, both the CA thickness and the temperature difference between the cooling liquid and the average CA temperature must be small. In the cooler shown in Figure 2B, heat is removed from the side surface of the CA by thermoelectric modules (note that heat can also be removed from the CA by using flowing liquid, gas, or spray). These modules can produce a temperature difference of up to 60°C between liquid and CA. This configuration, with 20°C liquid, allows a CA temperature in the −40→0°C range to be achieved, which is well suited to cooling the skin below 0°C. To achieve good heat transfer from the skin to the CA, thermal contact between the two must be excellent. This transfer is achieved by pressing the device firmly against the skin and by using a thin layer of high-thermal-conductivity liquid to fill in the skin microroughness. In this way, nearly ideal heat transfer can be achieved with solid contact coolers.

This study considers only the case of perfect sapphire-skin contact: imperfect contact has been described previously [12]. We believe the perfect contact case is of major theoretical interest because it demonstrates the ultimate potential of skin cooling. In practice, we can only approach perfect thermal contact. The skin cooler and method of application thereof should be developed to approach perfect contact. To approach perfect contact cooling, the sapphire surface should be flat, close contact between skin and sapphire must be achieved, and water or cream should be applied at the interface to aid thermal transfer.

For spray cooling (Fig. 2C), small drops of liquid with a boiling point below skin temperature are sprayed from an atomizer onto the skin. In principle, this process is similar to spraying water onto a hot griddle. Temperature of the drops depends on both the atomizer-skin distance and the ambient humidity. For a very small drop, the temperature is nearly at the boiling point of the fluid used (e.g., −26°C for TFE). When this very small drop lands on the skin, the drop boils and thus the temperature of the drop and the skin surface at the contact point remain close to the boiling point during evaporation. However, for large drops, temperatures can be much lower as the drop reaches the skin surface because of adiabatic expansion of the highly compressed liquid. The drops then form a liquid film, which begins to evaporate. The liquid layer thickness may be nonuniform, which produces different evaporation times across it. Thus, the dynamics of the spray contact layer are complex, and the cooling time can be longer than the actual spray pulse duration. For a liquid with a boiling point below 0°C, condensation and freezing of water also occurs at the skin surface. Ice crystals scatter light well and, therefore, can attenuate the laser treatment energy. Ambient air humidity and spray uniformity are important variables that should be controlled for efficient action.

For spray cooling, perfect contact does not have clear meaning because vaporization is a very dynamic process. In the theoretical section of this study, we assume ideal spray cooling where the skin surface temperature is equal to the boiling point of the liquid.

Laser pulse duration affects epidermal injury and modes of skin cooling. For a light-pulse duration less than the thermal relaxation time of a melanosome (≈1 μs), each melanosome can be heated independently [14]. For a light pulse duration longer than the time for heat propagation between melanosomes (≈50 μs), the epidermal region containing the melanosomes will be evenly heated. White, nontanned skin has melanosomes concentrated mainly in the 10-μm-thick basal layer, which is typically located 50–100 μm below the skin surface. Tanned or brown skin has both greater melanin content and more melanin distributed throughout the epidermis and stratum corneum. Tanning from ultraviolet exposure also causes epidermal thickening. Thus, thermal relaxation time of the absorbing epidermal layer (τ_a) can vary from ≈100 μs for white nontanned skin to as much as $\tau_a = \tau_e$ (epidermal relaxation time) ≈25 ms for a thick epidermis in the case of tanned or dark skin.

Cooling that occurs *during* the light pulse will hereafter be termed *parallel cooling*. Furthermore, we define two types of parallel cooling: *internal* and *external*. *Internal parallel cooling,* by which heat is conducted into the dermis, occurs when the light pulse duration is longer than τ_a (≈100 μs for light skin, ≈25 ms for dark/tanned skin). *External parallel cooling,* by which heat is conducted to the CA, requires a light pulse duration longer than τ_e (25 ms for both white and dark skin). For a light pulse duration longer than $\tau_e \approx$ 25 ms, the effect of parallel cooling becomes significant. We will show parallel cooling to be most effective for a light pulse duration longer than ≈100 ms. For pulses that have a duration much longer than τ_e, the effect of precooling is relatively insignificant and only parallel cooling is important. In the case of contact cooling, parallel cooling is easily performed. For spray cooling, this is also possible but more complicated, because of scattering of the incident light from the spray flow, a boiling liquid layer on the skin surface, and the need to avoid freezing the skin during prolonged spraying times.

The choice of cooling method also influences delivery of optical energy into the skin. Because of the refractive index mismatch between the skin surface and air, much of the back-scattered light undergoes total internal reflection (TIR) and contributes heavily to epidermal injury. Most of the light that experiences TIR dwells in the epidermis, since it is traveling at a small angle to the skin surface. The situation changes dramatically if a transparent thick medium with refractive index close to or greater than the skin surface refractive index (n ≈ 1.5) is placed in optical contact with skin during the light pulse. In this case, the TIR effect is spoiled and back-scattered light escapes, thereby reducing the radiance within the epidermis. We call this effect *optical damping*. Estimations made using diffusion theory show that the effect of optical damping produces a 1.5–1.7× decrease in basal layer radiance, an effect that decreases as the wavelength becomes shorter. When optical damping is present, there is also a radiance decrease in deeper skin layers, which reduces available light at the desired target. However, the effect is far more pronounced in the epidermis. When a sapphire contact cooler is used (Fig. 2A,B), near ideal conditions exist for optical damping. A thin liquid layer on the skin surface should be used with contact cooling. This layer also provides excellent optical coupling, which enhances the optical damping effect.

PRECOOLING

We assume that contact between the CA (spray or sapphire) and the skin is initiated within a few milliseconds. Under these conditions, the temperature distribution dynamics inside the skin are defined only by the skin surface temperature at the CA/skin interface. In the case of spray cooling, this interface temperature is equal to the liquid boiling point: $T_{surf} = T_{boil}$, which is the ideal case for spray cooling. In reality, $T_{surf} \leq T_{boil}$, because the spray may not be finely atomized or uniform. For contact cooling, the surface temperature remains constant during the entire contact period (see Appendix A) and is equal to

$$T_{surf} = \frac{T_{s0} + \chi \cdot T_0}{1 + \chi} \tag{1}$$

under ideal conditions. Here, $\chi = k_2/k_1 \cdot \sqrt{\alpha_1/\alpha_2}$, where k_1 (α_1) and k_2 (α_2) are the thermal conductivities (diffusivities) of the CA and the skin, respectively, and T_{s0} and T_0 are the initial temperatures of the CA and the skin before contact, respectively. For sapphire, χ is equal to approximately 0.09. Table 1 shows T_{surf} for five CA (air, water, fused silica, sapphire, and copper) in contact with T = 32°C skin. Only sapphire and copper maintain T_{surf} close to the initial CA temperature (i.e., prior to skin contact).

From equation (1), it follows that the temperature field dynamics in the skin under ideal

TABLE 1. Skin Surface Temperature for Various Materials Placed in Contact With 32°C Skin*

Initial CA temperature	Air[1]	Water	Fused silica	Sapphire	Copper
+10	31.89	19	18	12	11
0	31.84	13	12	3	1
−10	31.79	—	6	−5	−8
−26	31.70	—	−1	−17	−23
−50	31.58	—	−7	−37	−45

*Values in degrees Centigrade.
[1]No convection and moisture effects.

conditions are identical if the boiling point of the liquid T_{boil} and initial temperature of the contact cooler T_{s0} are linked by the following equation:

$$T_{s0} = T_{boil} - \chi \cdot (T_0 - T_{boil}). \quad (2)$$

For sapphire and initial epidermis temperature T = 32°C, this particular condition becomes

$$T_{s0} = T_{boil} - 0.09 \cdot (32°C - T_{boil}). \quad (3)$$

The effect of spray cooling using 1,1,1,2, TFE ($T_{boil} = -26°C$), therefore, should be the same as contact cooling with an initial sapphire temperature of $T_{s0} = -31°C$. *Thus, the theoretical treatment of spray and contact precooling under ideal conditions is exactly the same when equation (3) is satisfied.*

It should be noted that equation (3) does not take freezing into account. A more precise relation can be derived on the basis of equation (B8), which gives the relation between the skin surface temperature and the initial plate temperature when freezing of skin is allowed. Our calculations show that the difference between the precise relation and equation (3) is small for sapphire contact plates.

We now consider skin precooling for two different cases: (1) $T_{surf} > T_f$, where T_f is the freezing temperature of epidermal water, and (2) $T_{surf} < T_f$. We call the first case *soft cooling,* because epidermal cooling occurs without phase transition (ice formation). We call the second case *hard cooling,* because the epidermal surface layer freezes near the start of cooling and melts at the end of cooling. The theoretical analysis presented here uses a simplified model of the skin, which assumes 65% water content uniformly distributed throughout the epidermis. The concentration of salts and, therefore, the epidermal water freezing temperature are also assumed to be spatially uniform. In reality, the concentration of salts and water differ significantly for the stratum corneum, stratum granulosum, stratum spinosum, and basal layer. As discussed in the Introduction section, the real tissue freezing temperature is between 0 and −5°C. In our calculations, we have assumed $T_f = 0°C$.

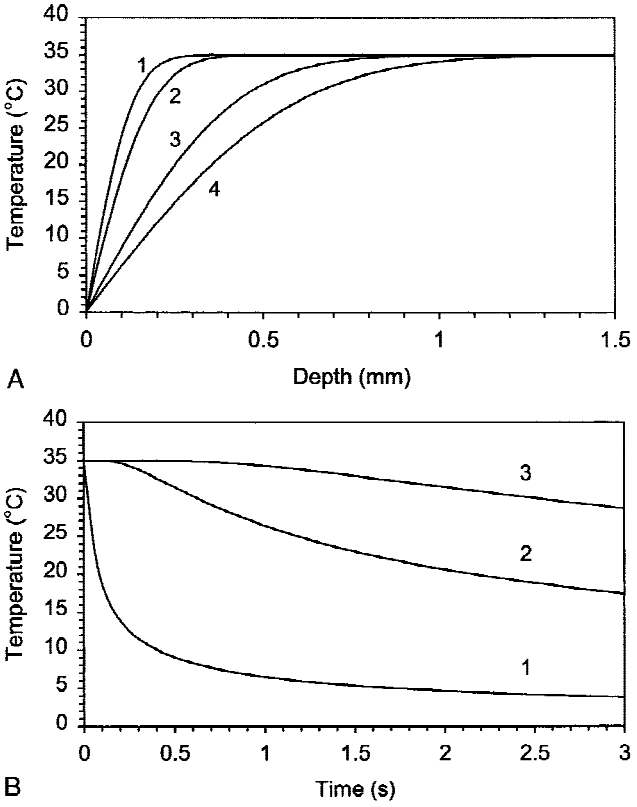

Fig. 3. **A:** Skin temperature versus depth for soft-mode precooling. The initial skin temperature is 35°C. The skin surface temperature is kept fixed at 0.1°C (e.g., by a sapphire contact plate at approximately −3°C). The precooling time is 50 ms (1), 100 ms (2), 500 ms (3), and 1000 ms (4). **B:** Skin temperature versus time at depths 0.1 mm (1), 0.5 mm (2), and 1 mm (3) for soft-mode precooling. The initial skin temperature is 35°C. The skin surface temperature is kept fixed at 0.1°C.

Soft-Precooling Mode ($T_{surf} > T_f$)

This cooling mode has been described previously [12]. Optimal soft-mode precooling is obtained when T_{s0} is chosen to produce $T_{surf} \approx T_f$. For sapphire, $T_{s0} \cong -3°C$ when $T_f = 0°C$. Figure 3A shows the temperature distribution inside the skin for four different sapphire/skin precooling times (50 ms, 100 ms, 500 ms, and 1000 ms) with a starting skin temperature of 35°C and $T_{surf} = 0.1°C$. As expected, longer precooling times produce lower temperatures at all skin depths. Figure 3B shows skin temperature at three different

depths beneath the surface (0.1 mm [basal layer], 0.5 mm [typical maximum depth of port wine vessels, range is 0.12–0.5 mm], and 1 mm [typical depth of hair follicle stem cells]) as a function of time for the same temperature conditions as Figure 3A. From Figure 3B, it follows that choosing the proper precooling time allows selective epidermal cooling. Thus, the ideal precooling time depends on the depth of the target structure. This dependence is described by a simple formula (see Appendix A):

$$t_{\text{opt}} = \frac{z_2^{\,2} - z_1^{\,2}}{4\alpha_2 \cdot \ln(z_2/z_1)}, \qquad (4)$$

where z_1 is the epidermal thickness, z_2 is the target-structure depth, and α_2 is the skin thermal diffusivity. At t_{opt}, the temperature difference between depths z_1 and z_2 has a maximum value, i.e., maximum cooling selectivity is obtained. At this time, the basal layer temperature is equal to

$$T_1 = T_{\text{surf}} + (T_0 - T_{\text{surf}}) \cdot \text{erf}\left(\frac{\ln(\delta)}{\delta^2 - 1}\right), \qquad (5)$$

with $\delta \equiv z_2/z_1$ and erf(x) being the error function. Note that the basal layer temperature (T_1) at t_{opt} is higher than the skin-surface temperature (T_{surf}) with the difference between them given by (following from equation (5))

$$(T_0 - T_{\text{surf}}) \cdot \text{erf}\left(\frac{\ln(\delta)}{\delta^2 - 1}\right). \qquad (6)$$

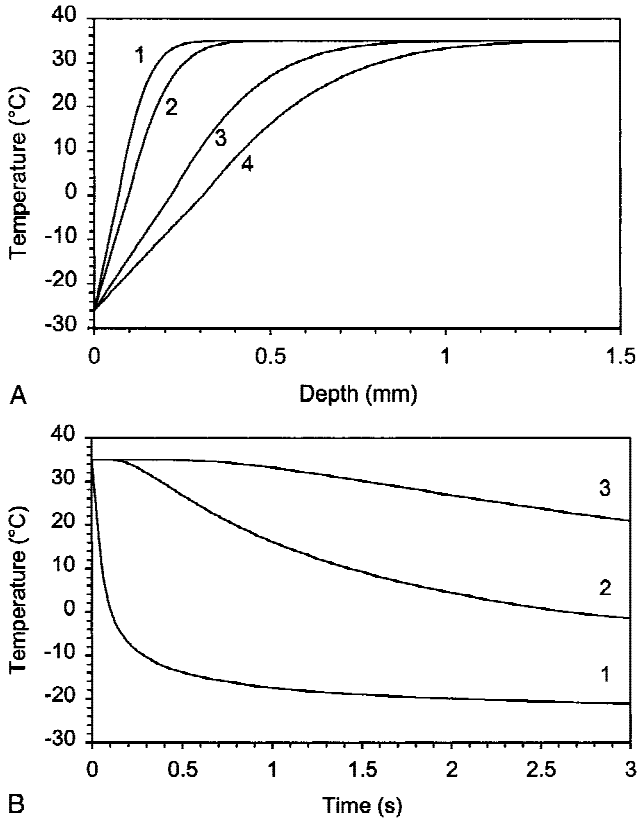

Fig. 4. **A:** Skin temperature versus depth for hard-mode precooling. The initial skin temperature is 35°C. The skin surface temperature is kept fixed at −26° (e.g., with tetrafluoroethane spray or with a sapphire contact plate at approximately −31°C). The precooling time is 50 ms (1), 100 ms (2), 500 ms (3), and 1000 ms (4). **B:** Skin temperature versus time at depths 0.1 mm (1), 0.5 mm (2), and 1 mm (3) for hard-mode precooling. The initial skin temperature is 35°C. The skin surface temperature is kept fixed at −26°C.

Hard-Precooling Mode ($T_{\text{surf}} < T_f$)

In the hard-precooling mode, freezing of the skin is allowed, and the cooling medium can be colder, e.g., $T_{\text{surf}} < 0$°C. *Skin freezing should provide additional protection from thermal injury during dermatologic laser procedures because a fraction of the laser energy absorbed in the epidermis will contribute to melting of the frozen layer.* Inside the skin, the depth of the border between frozen and nonfrozen skin is time dependent and moves deeper along with (but behind) the cooling front. We shall assume that a maximum epidermal freezing depth can be defined that does not result in acute skin damage, although the value has not yet been experimentally determined. Because the stratum corneum does not contain living cells, we assume its entire thickness can be frozen without any skin damage. In living tissue, two general types of low temperature injury may occur: cell injury caused by ice formation [2] and vascular stasis that develops after thawing [15]. The epidermis is better able to survive freezing and thawing than the dermis, especially when the temperature is just below the freezing point. The maximum allowable freezing depth is, therefore, in the 20–100 μm range. The model, which includes freezing and melting of water, is presented in Appendix B. All the results shown in this section were calculated by using this model and assume a starting skin temperature of 35°C.

Figure 4A shows calculated spatial temperature profiles inside the skin for four precooling times (50 ms, 100 ms, 500 ms, and 1000 ms) with $T_{\text{surf}} = -26$°C. Comparing these distributions to the analogous ones for soft-mode cooling (see Fig. 3A), two principal features can be seen. First, localized strong temperature gradients essentially

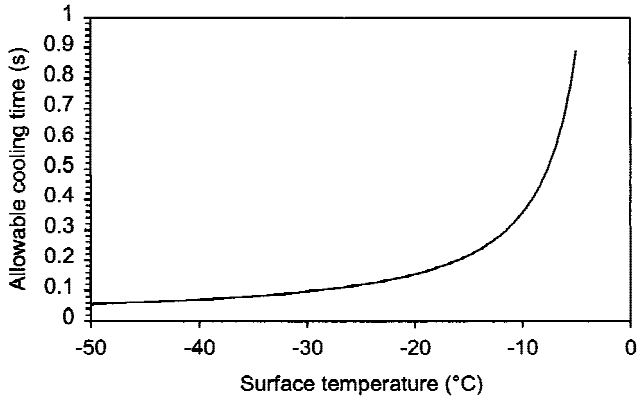

Fig. 5. Allowable cooling time versus surface temperature for hard-mode precooling. We assume the allowable cooling time to be the interval during which the frozen layer thickness reaches a predefined value of 100 μm.

coincide for the same precooling time (curve 2 in Figs. 3A, 4A). Second, freezing is present only in Figure 4A, as shown by the slight slope change at 0°C. Precooling times that exceed 100 ms will result in a frozen layer thickness >100 μm, which will cause epidermal injury. Figure 4B shows the time evolution of cooling at three depths (0.1 mm, 0.5 mm, and 1 mm) for $T_{surf} = -26$°C. Compared with the soft-cooling case (Fig. 3B), hard cooling provides greater selectivity: the temperature difference between the basal (0.1 mm) and target (0.5 mm, 1 mm) layers is larger at all times. Figure 5 shows the dependence of allowable cooling time on surface temperature where the frozen skin layer is limited to 100 μm. For a more conservative criteria of $z_f = 20$ μm, the allowable cooling time is <30 ms for the same surface temperature range shown in Figure 5.

Figure 6A and B shows the time evolution of temperature at the basal layer (0.1 mm) for three surface temperatures (curve 1: −50°C, curve 2: −26°C, and curve 3: 0.1°C) and two precooling times (100 ms and 500 ms, respectively). In this calculation, we have not limited the freezing depth. For curve 3 in both figures, the curve shape is relatively simple: a steep drop in temperature occurs during the precooling period followed by a gradual rise. Because the precooling time in Figure 6B is longer than 6A, the minimum temperature is lower. For curves 1 and 2, the behavior is more complex because of water freezing. Both curves exhibit a steep drop during the precooling period followed by a rapid rise to 0°C. The curves then plateau near 0°C while melting occurs. The combination of long precooling time and low temperature used in Figure 6B curve 1 results in a

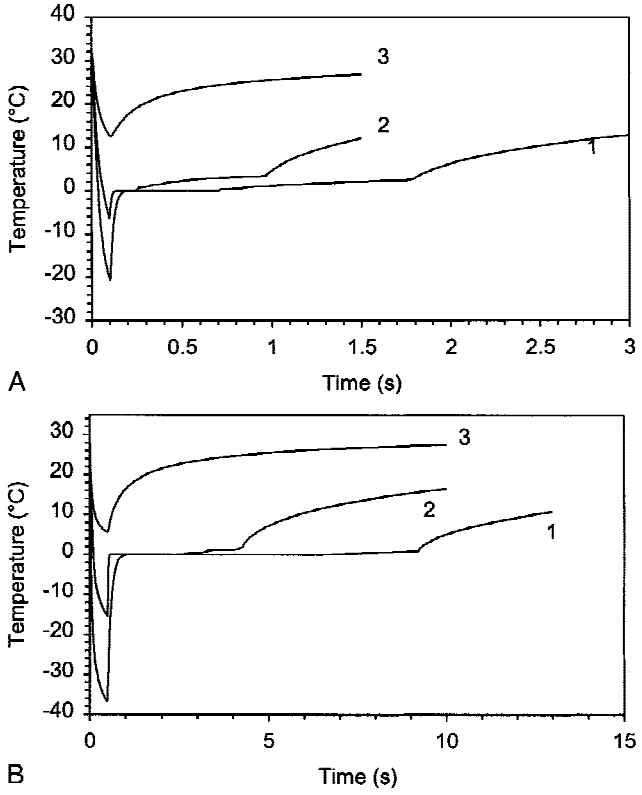

Fig. 6. **A,B:** Skin temperature at 100-μm depth versus time for hard-mode precooling. Initially, the skin surface temperature is kept constant for 100 ms (a) or 500 ms (b) at −50°C (1), −26°C (2), and 0.1°C (3) by thermal contact with the CA. The cooling agent is then removed at the end of the precooling time.

very thick frozen layer, which melts over a period of 8 seconds. This is the equivalent of cryogenic necrosis of the skin.

Because the hard-cooling mode uses a surface temperature below the freezing point of tissue, the duration must be carefully controlled to prevent irreversible damage to the epidermis. Compared with soft mode, hard mode provides: (1) faster cooling, (2) more selective cooling of epidermis, and (3) the opportunity to freeze the epidermis, which should provide additional protection from thermal injury.

Parallel Cooling

Parallel cooling, by definition, removes heat during a long light pulse. For effective parallel cooling, the light pulse duration should be longer than τ_e. Parallel cooling is highly effective for long exposure durations, as shown in the calculated curves presented in Figure 7. The figure shows skin temperature profiles at the end of the light pulse for four pulse durations without (curve 1,

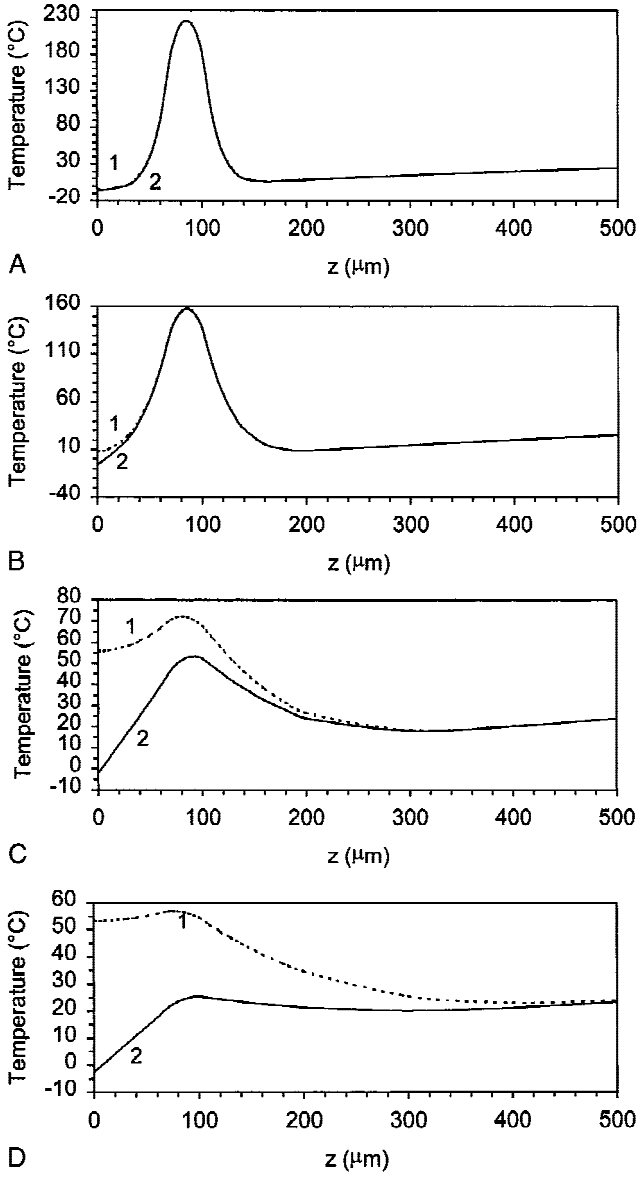

Fig. 7. Skin temperature versus depth at the end of an optical pulse at λ = 800 nm. Parallel cooling is turned off for the dashed curves (1) and is on for the solid ones (2). The pulsewidth is 3 ms (A), 10 ms (B), 100 ms (C), and 300 ms (D). The other parameters are input energy density 50 J/cm^2, 6-mm sapphire plate thickness, initial plate temperature −10°C, precooling time 1 second, initial skin temperature 35°C, effective basal layer thickness 30 μm (70 μm < z < 100 μm), basal layer optical density 0.02 (typical for white untanned skin). The thermal constants of the skin were determined using the empirical relations given by Takata et al. [17] with a water content of 65%.

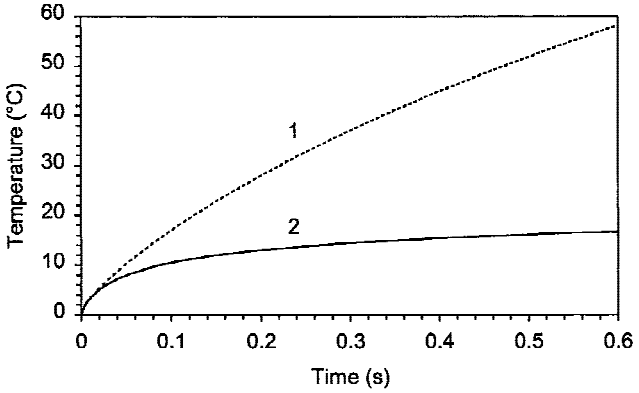

Fig. 8. Temperature at 100-μm depth versus time for a light pulse at λ = 800 nm. Parallel cooling is off for the top curve (1) and on for the bottom curve (2). The power density was 100 W/cm^2. All other parameters are the same as those in Figure 7.

dashed curve) and with (curve 2, solid curve) parallel cooling. The conditions used were −10°C sapphire, 1 second precooling time, untanned skin with 80-μm epidermal thickness, melanin layer optical density 0.02, λ = 800 nm (typical diode laser wavelength where water absorption is low) light with the same fluence F = 50 J/cm^2 delivered in four pulse durations: 3, 10, 100, and 300 ms. The calculation does not include phase transition (freezing). For short-pulse durations (Fig. 7A,B), parallel cooling is ineffective and only a small effect caused by internal parallel cooling can be seen. However, for pulses of >100-ms duration, it is highly effective because of external parallel cooling. For a 300-ms light pulse with parallel cooling (Fig. 7D), even the basal layer (z = 100 μm) temperature remains below normal body temperature. In Figure 8, the basal layer temperature is shown as a function of time for a power density of 100 W/cm^2 with (top dashed curve) and without (bottom solid curve) parallel cooling. Again, parallel cooling only becomes highly effective for pulse durations longer than ≈100 ms. For the extreme case, in which the light pulse duration is longer than the precooling time (0.2–1 s), parallel cooling provides essentially all of the epidermal protection. Heat transfer from epidermis to dermis partially offsets the effect of long cooling time in the case of parallel cooling. As we can see in Figure 7, the temperature at 0.5 mm depth is 26°C for a 3-ms pulse and 25°C for a 300-ms pulse. Thus, parallel cooling maintains selectivity in this case.

EXPERIMENTAL COMPARISON OF COOLING METHODS

Because precise measurement of temperature at the basal layer is not easily performed in

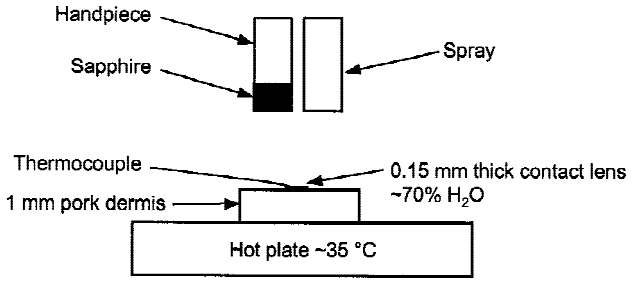

Fig. 9. Schematic diagram of the in vitro cooling experiment. The contact lens simulates the thermal properties of epidermis.

vivo, we designed an in vitro measurement to compare spray and contact cooling. The setup (Fig. 9) is similar to one previously used [12]. To simulate the epidermal layer, a 150-μm-thick hydrated ophthalmic contact lens with a hydration level of approximately 70% was used. The high hydration level of the contact lens results in thermal properties similar to epidermis. A 1-mm-thick piece of pork skin with the subcutaneous fat removed was used as the model dermis. The pork skin was maintained at ~35°C, with a thermocouple (Model IT-1E, bead size ~230 μm, Physitemp Instruments, Clifton, NJ) located between the pork skin and contact lens. For the contact cooling experiment, the sapphire-tipped handpiece of a commercially available laser hair removal system (E2000, Palomar Medical, Burlington, MA) was used. The 10-mm hexagonal sapphire tip was cooled to −27°C and pressed by hand against the contact lens/pork skin that was initially near body temperature. The spray cooling experiment used another commercially available laser hair removal system (GentleLase, Candela, Wayland, MA) that uses TFE for spray cooling before laser irradiation. The spray pulsewidth was set to the maximum 100-ms duration for this experiment. The thermocouple signal was fed into a Physitemp amplifier board. The output was digitized with a computerized data acquisition system operating at a sampling rate of 200 Hz. The thermocouple accuracy was ±0.1°C.

To measure the skin surface temperature during and after the 100-ms spray pulse, the thermocouple was placed on the skin surface without the contact lens. Figure 10 shows two typical trials. The temperature drops rapidly with constant slope during the spray pulse to a minimum value of −45 to −50°C. Because the liquid is not finely atomized and uniformly dispersed, a liquid layer forms on the surface. As the liquid layer is heated

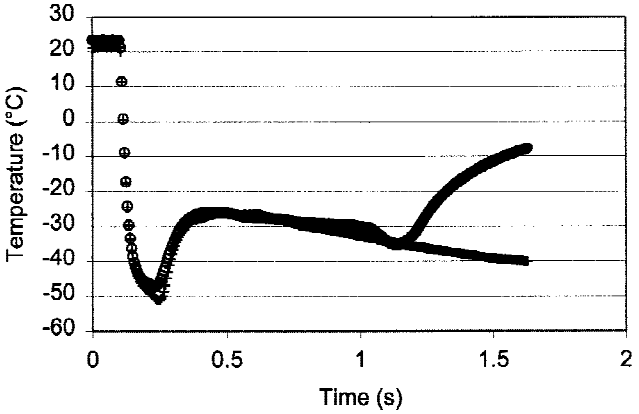

Fig. 10. Skin surface temperature for spray cooling with tetrafluoroethane. Spurt duration was set to 100 ms. Two trials are shown.

by the skin surface, the liquid begins to boil, which clamps the surface temperature near the −26°C boiling point. Even though the actual spurt duration is only 100 ms, the precooling time exceeds 500 ms.

Figure 11 shows the change in temperature of the simulated basal layer for three contact cooling trials and three spray cooling trials. In all three spray curves, the change in slope at t ~ 200 ms corresponds to the end of the 100-ms-duration spray pulse. The minimum basal layer temperature occurs approximately 200–500 ms after the end of the spray pulse. As shown in the previous figure, the boiling liquid layer maintains the surface temperature below −26°C for >500 ms, which causes the minimum temperature to occur long after the end of the 100-ms spray pulse. A 100-ms spray duration is the longest used at present in laser dermatology. As expected, the three contact-cooling curves are similar in shape to the theoretical curve shown in Figure 3B. The three contact-cooling curves fall steadily in temperature because the contact handpiece was kept in contact with the contact lens until t = 1.2 seconds. The shape of these curves is less complex than the spray-cooling curves, because the surface temperature remains fixed by the cooled sapphire block. For the contact cooling curves, changes in the contact pressure may account for the differences observed, whereas variations in the three spray-cooling curves probably arise from thickness nonuniformity in the sprayed layer. Nevertheless, both cooling methods produced significant cooling of the simulated basal layer to between −5 and +5°C, about 500 ms after commencement of cooling.

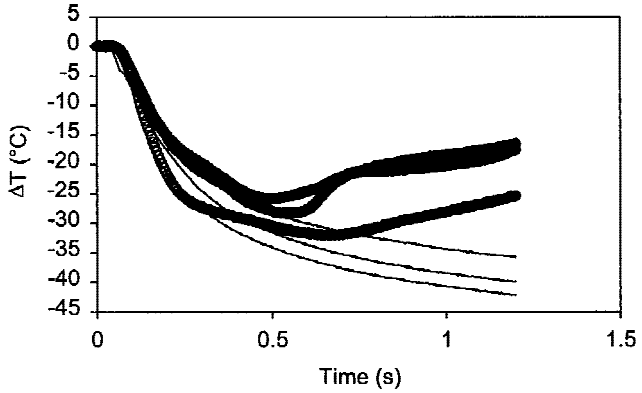

Fig. 11. Simulated basal layer temperature change for spray (thick curves) and contact (thin curves) cooling. Three trials for each cooling method are shown.

CONCLUSIONS

1. Both methods remove heat from the skin by contact.
2. Under ideal conditions, both precooling methods produce the same spatial temperature distribution inside the skin if the skin surface temperature is the same.
3. Both methods require control of precooling time to achieve selectivity and, for hard mode, prevent irreversible epidermal damage caused by freezing. The precooling time for spray can be much longer than the spurt duration and cannot be easily controlled. Precooling time for the contact case can be controlled by monitoring heating of the sapphire plate [12].
4. The protective effect of spray cooling results from epidermal precooling before a light pulse.
5. For optimum spray cooling, based on thermal considerations, the laser should be fired when the basal layer temperature is minimum, not at the end of the spurt. Scattering of the laser light may also affect choice of delay time, but we did not study this factor.
6. The protective effect of contact cooling results from epidermal precooling before a light pulse and cooling in parallel with the light pulse for pulse durations >100 ms.
7. Contact with a sapphire plate causes optical damping (spoiling of total internal reflection at the skin surface), which tends to optically spare the epidermis.
8. Contact cooling requires good thermal and optical contact between the CA and the skin. A transparent liquid with good thermal conductivity can be used to maximize epidermal protection.

Our analysis of soft-mode cooling ($T_{surf} > T_f$) shows:

1. This mode is most effective when T_{surf} is only slightly higher than T_f.
2. Epidermal injury caused by freezing is not possible.
3. The depth of cooling is unlimited.
4. The minimum epidermal temperature is limited to 4–10°C (T_f = 0°C), and relatively long precooling times (0.5–3 seconds) are required to achieve these values.

Our analysis of hard-mode cooling ($T_{surf} < T_f$) shows:

1. Additional epidermal protection can be achieved by creating a frozen skin layer.
2. Compared with soft-mode, hard-mode cooling is faster and more selective.
3. The precooling time must be carefully controlled to prevent irreversible epidermal damage caused by freezing.
4. Because the precooling time must be limited, the cooling depth is also limited.

For light pulses shorter than τ_e, both spray and contact cooling methods produce equivalent temperature distributions before the laser pulse, if the skin surface temperature is the same during the precooling procedure. For pulses longer than τ_e (>100 ms), contact cooling is superior to a –26°C cryogen spray because of parallel cooling. Some practical issues in choosing spray vs. contact for precooling include the following. (i) *Physical compression of the tissue,* which collapses blood vessels, stretches the skin, and often decreases its thickness. Compression is impractical with spray cooling and difficult to avoid with contact cooling. Compression increases thermal contact in the case of contact cooling. For vascular skin lesions such as port wine stains, strong compression is undesirable and spray precooling is probably a better choice. For targets such as hair follicles, contact cooling with strong compression may be a better choice. (ii) *Cost,* which includes both equipment and disposable supplies. (iii) Finally, *safety and ergonomic factors* can be considered. If either the spray or contact fails, the epidermis may suffer some harm, but the modes of failure are likely to be different. A potential safety hazard may also

exist if cryogen spray is used near the eyes, because the cornea lacks a stratum corneum.

The skin "does not care" which external medium is used to extract heat; it is the combination of skin surface temperature and time of the heat extraction that determines the extent of skin cooling. Both spray and contact-cooling methods can effectively precool the epidermis before arrival of a short (<20 ms) laser pulse. To avoid freeze injury, the ideal temperature for the external cooling medium is near −5°C for 1-second precooling time. For longer pulse duration (>100 ms), significant heat extraction during the light pulse (parallel cooling) becomes possible. Contact devices provide parallel cooling much more easily than cryogen sprays, while cryogen sprays easily provide short, aggressive precooling. In some applications, compression of the skin by a contact-cooling device is desired, whereas spray cooling may be more appropriate for vascular lesions.

REFERENCES

1. Sherman J. Survival of higher animal cells after the formation and dissolution of intracellular ice. Anat Rec 1962;144:171–189.
2. Rand R, Rinfret V, Von Leden H. Cryobiology-some fundamentals in surgical context. In: Cryosurgery. Springfield: Charles C Tomas; 1968. p 19–31.
3. Wheeland RG. Cutaneous surgery. Philadelphia: WB Saunders; 1994.
4. Dierickx C, Grossman MC, Farinelli WA, Anderson RR. Permanent hair removal by normal-mode ruby laser. Arch Dermatol 1998;134:837–842.
5. Gilchrest BA, Rosen S, Noe JN. Chilling port wine stains improves the response to argon laser therapy. Plast Reconstr Surg 1982;69:278–283.
6. Nelson JS, Milner TE, Anvari B, Tanenbaum BS, Kimel S, Svaasand LO, Jacques SL. Dynamic epidermal cooling during pulsed laser treatment of port wine stain: a new methodology with preliminary clinical evaluation. Arch Dermatol 1995;131:695–700.
7. Milner TE, Anvari B, Keikhanzadeh K, Dave D, Nelson JS. Analysis of nonablative skin resurfacing. Proc SPIE 1997;2970:367–373.
8. Anvari B, Milner TE, Tanenbaum BS, Kimel S, Svaasand LO, Nelson JS. Selective cooling of biological tissues: application for thermally mediated therapeutic procedures. Phys Med Biol 1995;40:241–252.
9. Anvari B, Milner TE, Tanenbaum BS, Kimel S, Svaasand LO, Nelson JS. A theoretical study of the thermal response of skin to cryogen cooling and pulsed laser irradiation: implications for the treatment of port wine stain. Phys Med Biol 1995;40:1451–1465.
10. Anvari B, Ver Steeg BJ, Milner TE, Tanenbaum BS, Klein TJ, Gerstner E, Kimel S, Nelson JS. Cryogen spray cooling of human skin: effects of humidity level, spraying distance, and cryogen boiling point. Proc SPIE 1997; 3192:106–110.
11. Torres JH, Anvari B, Milner TE, Tanenbaum BS, Milner TE, Yu JC, Nelson JS. Internal temperature measurements in response to cryogen spray cooling of a skin phantom. Proc SPIE 1999;3590:11–19.
12. Altshuler GB, Zenzie HH, Erofeev AV, Smirnov MZ, Anderson RR, Dierickx C. Contact cooling of the skin. Phys Med Biol 1999;44:1003–1023.
13. Anvari B, Milner TE, Tanenbaum BS, Nelson JS. A comparative study of human skin thermal response to sapphire contact and cryogen spray cooling. IEEE Trans Biomed Eng 1998;45:934–941.
14. Anderson RR, Parrish JA. Selective photothermolysis: precise microsurgery by selective absorption of pulsed radiation. Science 1983;220:524–527.
15. Kreyberg L. Stasis and necrosis. Scand J Clin Lab Invest 1963;15:1–9.
16. Carslaw HS, Jaeger JC. Conduction of heat in solid. Oxford: Clarendon press; 1959.
17. Takata AN, Zaneveld L, Richter W. Laser induced thermal damage in skin. Report SAM-TR-77-38 Brooks Air Force Base, TX: US Air Force School of Aerospace Medicine; 1977.
18. Tikhonov NA, Samarski AA. Equations of mathematical physics. Moscow: Nauka; 1977.
19. Dulnev GN, Zarichnyk YP. Thermal conductivity of mix and composite materials. Leningrad: Energia; 1974.

APPENDIX A

We consider herein the temperature dynamics within the skin for the case where no freezing occurs. To prevent freezing, the surface temperature T_{surf} should not fall below the freezing point $T_f \approx 0°C$. This type of cooling will be referred to as soft mode in contrast to hard mode, for which the upper part of the skin becomes frozen.

First, let us consider sapphire plate cooling (Fig. 12B). Given appropriate thermal coefficients, other solid or liquid contact-cooling agents can also be modeled using the theory presented here. The spatial and time evolution of the sapphire temperature $T_1(z,t)(z < 0)$ and the skin temperature $T_2(z,t)(z \geqslant 0)$ is governed by the following set of heat conduction equations [16]:

$$\begin{aligned} \frac{\partial T_1}{\partial t} &= \alpha_1 \cdot \frac{\partial^2 T_1}{\partial z^2}, z < 0, \\ \frac{\partial T_2}{\partial t} &= \alpha_2 \cdot \frac{\partial^2 T_2}{\partial z^2}, z \geqslant 0, \end{aligned} \quad (A1)$$

with α_1 and α_2 equal to the thermal diffusivities of the sapphire and the skin, respectively. The initial conditions are

$$\begin{aligned} T_1(z,0) &= T_{s0}, z < 0, \\ T_2(z,0) &= T_0, z \geqslant 0, \end{aligned} \quad (A2)$$

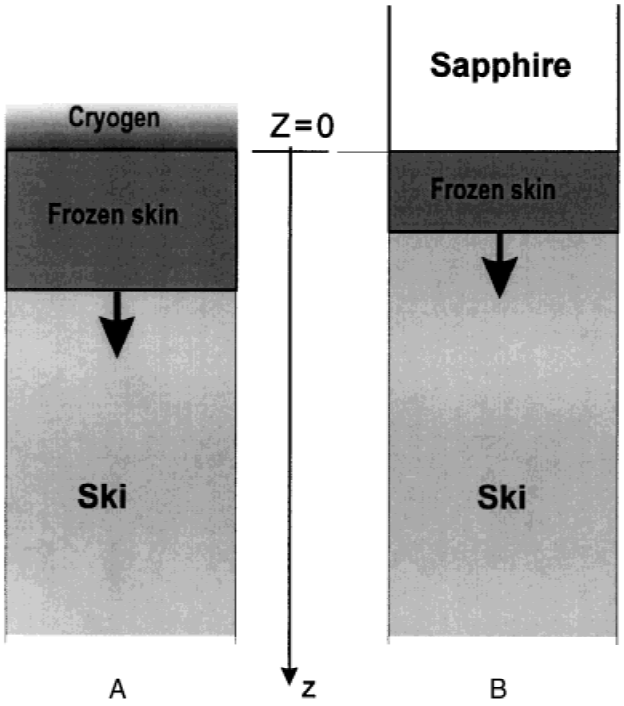

Fig. 12. Coordinate system for spray (**A**) and contact plate (**B**) skin cooling methods.

where T_{s0} and T_0 are the initial temperatures of the sapphire and the skin, respectively. Assuming perfect thermal contact between the sapphire and the skin (for treatment of imperfect contact, see Altshuler et al. [12]), the boundary conditions take the form

$$T_1(-\infty,t) = T_{s0},\ T_2(+\infty,t) = T_0, \qquad \text{(A3)}$$
$$T_1(0,t) = T_2(0,t),\ k_1 \cdot \frac{\partial}{\partial z} T_1(0,t) = k_2 \cdot \frac{\partial}{\partial z} T_2(0,t),$$

with k_1 and k_2 equal to the thermal conductivities of the sapphire and the skin, respectively. Let us note that equation (A3) is rigorous and is applicable with no limitations other than ideal thermal contact. Moreover, the same condition may be used in the case of imperfect contact [12]. However, in the latter case the two-layer model has to be transformed into a three-layer one that has to include a third layer of thickness d with thermal conductivity κ_3 to separate the sapphire and the skin. Then, the heat conduction problem inclusive of the intermediate layer can be solved exactly for the boundary conditions given by equation (A3) [12]. The above description of contact cooling seems to be the most appropriate for the problem under consideration.

In Anvari et al. [13], the authors used the Robin boundary condition

$$\kappa_2 \frac{\partial}{\partial z} T_2(0,t) = H \cdot (T_2(0,t) - T_{s0}) \qquad \text{(A4)}$$

to simulate sapphire contact cooling of the skin, with H being the coefficient of surface heat transfer. To apply the Robin boundary condition in the case of dynamic skin cooling, it is necessary to have the relaxation time of the contact layer between sapphire and skin less than the epidermal relaxation time (10–13 ms). If the above condition is not met, H cannot be treated as a fixed value. Using boundary condition equation (A3), it is straightforward to derive the following expression for *H:*

$$H = \frac{\kappa_3}{d}. \qquad \text{(A5)}$$

To evaluate the surface heat transfer coefficient, Anvari et al. [13] have compared the experimental temperature distribution in skin with those obtained numerically with the use of the Robin boundary condition. They have found that the value of H varies from $H_1 = 0.2$ W/(cm^2 K) to $H_2 = 1$ W/(cm^2 K). To interpret these results, let us assume the contact layer to be a water film or an air-filled space. Therefore, from equation (A5), the water film (air-filled space) must be from 60 μm (2.6 μm) to 300 (13.1 μm) thick. The relaxation time $\tau = d^2/2\alpha$ varies from about 2.6 ms (1.7×10^{-4} ms) to approximately 310 ms (4.2×10^{-3} ms) in the water film case (air-filled space). Therefore, the Robin boundary condition seems to have limited application in this case. Specifically, it is applicable to the air-filled space and may not be used for the water film. For very good thermal contact, the Robin boundary condition requires $T_2(0,t) = T_{s0}$. This is not consistent with the surface temperature given by equation (A8).

It is straightforward to prove that the solution for the equation set (A1)–(A3) is

$$T_1(z,t) = T_{surf} + (T_{surf} - T_{s0}) \cdot \mathrm{erf}\left(\frac{z}{2\sqrt{\alpha_1 t}}\right), \quad z < 0, \qquad \text{(A6)}$$

$$T_2(z,t) = T_{surf} + (T_0 - T_{surf}) \cdot \mathrm{erf}\left(\frac{z}{2\sqrt{\alpha_2 t}}\right), \quad z \geq 0, \qquad \text{(A7)}$$

where the surface temperature is given by

$$T_{surf} = \frac{T_{s0} + \chi \cdot T_0}{1 + \chi}, \chi \equiv \frac{k_2}{k_1} \cdot \sqrt{\frac{\alpha_1}{\alpha_2}}, \quad \text{(A8)}$$

and $\mathrm{erf}(\xi) = 2/\sqrt{\pi} \cdot \int_0^{\xi} \exp(-\eta^2)\, d\eta$ is the error function.

Thus, when the sapphire plate and the skin are brought into perfect thermal contact, both the contact surface temperatures jump instantaneously to T_{surf}. Then, these temperatures are kept fixed during the cooling procedure.

Now, let us turn to spray cooling (Fig. 12A). Similar to sapphire plate cooling, we assume perfect thermal contact between the skin and the spray. The surface temperature of the skin T_{surf} is equal to the boiling temperature of the cryogen until the spray boils away. Meanwhile, the temperature distribution in the skin is still governed by equation (A5).

Upon contact with skin, the spray drops may have a temperature equal to or less than T_{boil}. In the contact zone, the liquid begins to boil and its temperature remains constant until evaporation occurs. As stated earlier, the boiling liquid may remain on the skin surface for a time period that is significantly longer than the spurt duration. Thus, at the start of the spray treatment, the skin-surface temperature may be below the boiling point. At some point after the spray spurt ends, the liquid boils, and the skin surface temperature is clamped at T_{boil} until the liquid evaporates. To model this process, the Dirichlet boundary condition, in which the skin surface temperature is fixed, is the most appropriate. As a first approximation, we can assume $T_{surf} = T_{boil}$. In a more rigorous treatment, T_{surf} as a function of time can be given by a function similar to that shown in Fig. 10. In this case, the temperature measured by a thermocouple in contact with the skin may differ from the actual skin-surface temperature. In our opinion, this approach would accurately model the actual spray-cooling process. In references 8, 9, 11, and 13, the Robin boundary condition was used to describe spray cooling. We believe it is not applicable for this particular case for the following reasons. First, thermal contact between the spray drops/liquid layer and skin changes continuously and significantly during spray cooling. Initially, spray drops form a liquid layer and air bubbles form by boiling liquid. Next, intensive boiling occurs, which can then be followed by liquid flowing along the skin surface. In this case, it is very difficult to define whether perfect or imperfect contact is taking place between the thin layer of vaporizing liquid and skin. Thus, the coefficient of surface heat transfer cannot be assumed to be constant. Second, the spray temperature changes continuously and significantly as well, as shown in the experimental graph (Fig. 10). Therefore, the CA temperature cannot be assumed to be constant in equation (A4). For these reasons, in different papers we find significantly different values of surface heat transfer coefficient and cryogen film temperature (compare references 9 and 13 with 11).

The optimal cooling time may be evaluated in the following manner: let z_1 and z_2 be the depths of the basal layer and the specified target, respectively. We assume both depths are positive and $z_1 < z_2$. The temperature difference $\Delta T(t) \equiv T(z_2,t) - T(z_1,t)$ is zero at $t = 0$, because both the temperatures are equal to T_0. At the initial stage of the cooling procedure, $T(z_1,t)$ falls abruptly, whereas $T(z_2,t)$ is kept almost fixed. However, when the cold front reaches the target depth, the latter temperature starts to decrease. Meanwhile, the former temperature reaches its steady state value and stops changing. It follows from the above argument that the temperature difference should be a maximum at a certain time t_{opt}, which is the optimal cooling time. Based on equation (A5), one can show that t_{opt} depends neither on the procedure type (sapphire plate or spray cooling) nor the surface temperature and is given by

$$t_{opt} = \frac{z_2^2 - z_1^2}{4\alpha_2 \cdot \ln\left(\frac{z_2}{z_1}\right)}. \quad \text{(A9)}$$

Finally, we consider the dependence of skin-layer thermal constants on water content, W. Generally the human skin contains 65–75% water. To calculate the thermal constants, we use the following empirical formulas [17]

$$\begin{aligned} \rho &= (1.3 - 0.3 \cdot W)\, \frac{\mathrm{g}}{\mathrm{cm}^3}, \\ c &= 4.18 \cdot \left(0.37 + 0.67 \cdot \frac{W}{\rho}\right) \frac{\mathrm{J}}{\mathrm{g} \cdot {}^0C}, \\ \alpha &= \left(0.1333 + 1.36 \cdot \frac{W}{\rho}\right) \cdot 10^{-3}\, \frac{\mathrm{cm}^2}{\mathrm{s}}, \\ \kappa &= \alpha \cdot \rho \cdot c. \end{aligned} \quad \text{(A10)}$$

APPENDIX B

In this Appendix, we present the mathematical model for hard-mode cooling. Consider the sapphire plate cooling schematic depicted in Figure 12B.

Let $T_1(z,t)$, $(z < 0)$; $T_2(z,t)$, $(0 \le < \xi(t))$; and $T_3(z,t)$, $(z \ge \xi(t))$ be the temperatures of the sapphire plate, the frozen skin layer, and the remainder of the skin, respectively, with $\xi(t)$ representing the frozen-layer thickness. The heat conduction equations and the initial and boundary conditions may be written as follows:

$$\begin{aligned}
\frac{\partial T_1}{\partial t} &= \alpha_1 \cdot \frac{\partial^2 T_1}{\partial z^2}, z < 0,\\
\frac{\partial T_2}{\partial t} &= \alpha_2 \cdot \frac{\partial^2 T_2}{\partial z^2}, 0 \le z < \xi(t),\\
\frac{\partial T_3}{\partial t} &= \alpha_3 \cdot \frac{\partial^2 T_3}{\partial z^2}, z \ge \xi(t),
\end{aligned} \tag{B1}$$

$$\begin{aligned}
T_1(z,0) &= T_{s0}, z < 0,\\
T_3(z,0) &= T_0, z \ge \xi(t),
\end{aligned} \tag{B2}$$

$$\begin{aligned}
T_1(-\infty,t) &= T_{s0}, T_3(+\infty,t) = T_0,\\
T_1(0,t) &= T_2(0,t), k_1 \cdot \frac{\partial}{\partial z} T_1(0,t)\\
&= k_2 \cdot \frac{\partial}{\partial z} T_2(0,t),\\
T_2(\xi(t),t) &= T_3(\xi(t),t) = T_f,\\
k_2 \cdot \frac{\partial}{\partial z} T_2(\xi(t),t) &- k_3 \cdot \frac{\partial}{\partial z} T_3(\xi(t),t) = \lambda \cdot \rho \cdot \frac{d\,\xi(t)}{d\,t}.
\end{aligned} \tag{B3}$$

Here, the variables labeled by indices 1, 2, 3 refer to the sapphire, the frozen skin, and the normal skin, respectively; T_{s0} and T_0 are the initial temperatures of the sapphire plate and the skin, respectively; T_f is the freezing point of the skin; ρ is the density of the skin; and λ is the specific melting heat of the frozen skin. Equations (B1)–(B3) describe a modified Stephan problem [18]. We have applied the similitude method to get the following solution for the equation set (B1)–(B3)

$$T_1(z,t) = T_{surf} + (T_{surf} - T_{s0}) \cdot \mathrm{erf}\left(\frac{z}{2\sqrt{\alpha_1 t}}\right), z < 0, \tag{B4}$$

$$T_2(z,t) = T_{surf} + B_2 \cdot \mathrm{erf}\left(\frac{z}{2\sqrt{\alpha_2 t}}\right), 0 \le z < \xi(t), \tag{B5}$$

$$T_3(z,t) = T_0 - B_3 \cdot \mathrm{erfc}\left(\frac{z}{2\sqrt{\alpha_3 t}}\right), \xi(t) \le z < +\infty, \tag{B6}$$

$$\xi(t) = \beta \cdot \sqrt{t}, \tag{B7}$$

where the eigenvalue β determines the expansion rate of the frozen layer. Here, $\mathrm{erfc}(x) \equiv 1 - \mathrm{erf}(x)$ is the complementary error function, and T_{surf} is the temperature of the skin/sapphire plate interface given by

$$T_{surf} = T_f - \frac{\sigma_1}{1+\sigma_1} \cdot (T_f - T_{s0}), \tag{B8}$$

with $\chi \equiv (k_1/k_2) \cdot \sqrt{\alpha_2/\alpha_1}$, $\sigma_1 \equiv \chi \cdot \mathrm{erf}(\beta/(2\sqrt{\alpha_2}))$. Coefficients B_2 and B_3 are

$$B_2 = \frac{T_f - T_{surf}}{\mathrm{erf}(\beta/(2\sqrt{\alpha_2}))}, B_3 = \frac{T_0 - T_f}{\mathrm{erfc}(\beta/(2\sqrt{\alpha_3}))}. \tag{B9}$$

Finally, the eigenvalue β is the solution of the following characteristic equation:

$$\begin{aligned}
\frac{\sqrt{\pi}}{2}\lambda\rho\beta &+ \frac{k_1}{\sqrt{\alpha_1}} \cdot \frac{\exp\left(-\frac{\beta^2}{4\alpha_2}\right) \cdot (T_{s0} - T_f)}{1 + \sigma \cdot \mathrm{erf}\left(\frac{\beta}{2\sqrt{\alpha_2}}\right)}\\
&+ \frac{k_3}{\sqrt{\alpha_3}} \cdot \frac{\exp\left(-\frac{\beta^2}{4\alpha_3}\right) \cdot (T_0 - T_f)}{1 - \mathrm{erf}\left(\frac{\beta}{2\sqrt{\alpha_3}}\right)} = 0.
\end{aligned} \tag{B10}$$

The transcendent equation (B10) has a positive solution, provided the initial temperature of the sapphire plate T_{s0} lies below a certain threshold temperature, T_{crit}, which may be called the critical temperature for skin freezing

$$T_{s0} < T_{crit} = T_f \cdot (1+\gamma) - \gamma \cdot T_0, \tag{B11}$$

where $\gamma = k_3/k_1 \cdot \sqrt{\alpha_1/\alpha_3}$.

When equation (B11) is satisfied, the skin starts to freeze; therefore, the cooling proceeds in hard mode. At the instant thermal contact between the skin and the sapphire plate is established, the contact-plane temperature jumps to T_{surf}, which remains constant during the cooling

procedure. Meanwhile, the frozen-layer thickness grows as shown by equation (B7).

Let us now turn to spray cooling. Because we assume perfect contact between the skin and the spray, the value of T_{surf} is now equal to the spray boiling temperature. Equation set (B5)–(B7), which give the temperature distribution inside the skin and the frozen-layer thickness, still apply. However, the characteristic equation changes to

$$\frac{\sqrt{\pi}}{2}\lambda\rho\beta + \frac{k_2}{\sqrt{\alpha_2}} \cdot \frac{\exp\left(-\frac{\beta^2}{4\alpha_2}\right) \cdot (T_{surf} - T_f)}{\operatorname{erf}\left(\frac{\beta}{2\sqrt{\alpha_2}}\right)} + \frac{k_3}{\sqrt{\alpha_3}} \cdot \frac{\exp\left(-\frac{\beta^2}{4\alpha_3}\right) \cdot (T_0 - T_f)}{1 - \operatorname{erf}\left(\frac{\beta}{2\sqrt{\alpha_3}}\right)} = 0. \quad \text{(B12)}$$

Finally, the condition under which the cooling proceeds in the hard mode is simply $T_{surf} < T_f$.

The main drawbacks of the above analytical models are as follows:

1. The models do not allow for the thawing process that starts when the sapphire plate is removed from the skin surface or the spray boils away.
2. The models do not include imperfect thermal contact that can occur in clinical skin cooling procedures.
3. Both the models assume infinite thickness of the skin and the plate. As a result, the temperature at the contact plane seems to show no variation in time. In practice, however, such variations should occur due to the finite plate thickness and the effect of blood vessels.

For these reasons, we have also developed a numeric model that uses the finite difference technique to solve the heat conduction problem for skin of finite thickness. The latter model allows for both freezing and thawing.

The equations describing the model are the same as listed above except for the boundary conditions. At the end of the cooling procedure, the boundary condition at the skin surface changes so that the heat flux through the surface becomes zero. Furthermore, the temperature at the depth of the blood vessels (3–5 mm under the surface) is assumed to be constant in time.

The numeric model uses the conservative finite difference method to calculate the temperature distribution within the skin and the position of the phase interface. The skin bulk is divided into cells, and the heat fluxes amon the cells are evaluated using the Fourier law. Each cell may be in three possible states: normal, intermediate, and frozen. If the temperature of the normal cell falls below T_f or the temperature of the frozen cell exceeds T_f, then the phase transition starts and the cell passes into the intermediate state. In the latter state, the cell temperature is kept fixed at T_f, and variations in the heat quantity within the cell result in changes in the degree of freezing. The above variations of heat quantity are due to heat generation within the cell and the heat exchange between the cell and its neighbors. When the degree of freezing falls below zero or rises above 1, the cell passes into the normal or frozen state, respectively. The thermal constants of the cell in the intermediate state are reevaluated by weighted averaging of those of ice and the dehydrated skin residue each time the degree of freezing changes.

To evaluate the thermal conductivity (κ_f) of the frozen layer, we apply the formalism of generated conductivity developed by Dulnev and Zarichnyk [19]. We assume the frozen skin to consist of two components penetrating deeply into each other. The first component is ice and the second one is dehydrated skin residue. The thermal constants of the latter component are determined by equation (A10) with $W = 0$. The thermal conductivity of the composite frozen skin is given by the following relation [19]:

$$\kappa_f = \kappa_{ice} \cdot \left[C^2 + v \cdot (1 - C)^2 + \frac{2vC(1 - C)}{vC + 1 - C} \right]; v \equiv \frac{\kappa_{res}}{\kappa_{ice}}, \quad \text{(B13)}$$

where κ_{ice} and κ_{res} are the thermal conductivities of the ice and the residue, respectively. Parameter C is found from the relation

$$C = 0.5 - \cos\left(\frac{2 \cdot \pi - \arccos(1 - 2 \cdot m_2)}{3}\right), m_2 < 0.5, \quad \text{(B14)}$$

with $m_2 \approx 1 - W$ being the volume fraction of the skin residue in the composite frozen skin. Then, the specific heat of the frozen skin is given by $c_f = W \cdot c_{ice} + (1 - W) \cdot c_{res}$, and the density of the frozen skin is set to be equal to that of the normal skin $\rho_f = \rho$.